Journal of Volcanology and Geothermal Research 320 (2016) 100–106

Contents lists available at ScienceDirect

Journal of Volcanology and Geothermal Research

journal homepage: www.elsevier.com/locate/jvolgeores

Volcán de Colima dome collapse of July, 2015 and associated pyroclastic density currents

Gabriel A. Reyes-Dávila [a], Raúl Arámbula-Mendoza [a,*], Ramón Espinasa-Pereña [b], Matthew J. Pankhurst [c], Carlos Navarro-Ochoa [a], Ivan Savov [c], Dulce M. Vargas-Bracamontes [d], Abel Cortés-Cortés [a], Carlos Gutiérrez-Martínez [b], Carlos Valdés-González [b], Tonatiuh Domínguez-Reyes [a], Miguel González-Amezcua [a], Alejandro Martínez-Fierros [a], Carlos Ariel Ramírez-Vázquez [a], Lucio Cárdenas-González [b], Elizabeth Castañeda-Bastida [b], Diana M. Vázquez Espinoza de los Monteros [b], Amiel Nieto-Torres [b], Robin Campion [e], Loic Courtois [f,g], Peter D. Lee [f,g]

[a] Centro Universitario de Estudios e Investigaciones en Vulcanología (CUEIV), Universidad de Colima, Av. Bernal Díaz del Castillo No. 340, Col. Villas San Sebastián, C.P. 28045, Colima, Colima, Mexico
[b] Centro Nacional de Prevención de Desastres (CENAPRED), Av. Delfín Madrigal No. 665, Col. Pedregal de Santo Domingo, Del. Coyoacán, C.P. 04360, Ciudad de México, Mexico
[c] School of Earth and Environment, University of Leeds, Leeds LS2 9JT, UK
[d] Cátedras CONACYT at CUEIV, Universidad de Colima, Av. Bernal Díaz del Castillo No. 340, Col. Villas San Sebastián, C.P. 28045, Colima, Colima, Mexico
[e] Instituto de Geofísica, Universidad Nacional Autónoma de México, Circuito Científico, s.n. Coyoacán, C.P. 04510, D.F., Mexico
[f] Manchester X-ray Imaging Facility, School of Materials, The University of Manchester, Manchester, M13 9PL, UK
[g] Research Complex at Harwell, Rutherford Appleton Laboratories, Didcot OX11 0FA, UK

ARTICLE INFO

Article history:
Received 7 October 2015
Received in revised form 8 April 2016
Accepted 11 April 2016
Available online 16 April 2016

Keywords:
Monitoring
Volcán de Colima
Petrology
Lava dome collapse
Boiling-over
Pyroclastic density currents

ABSTRACT

During July 10th–11th 2015, Volcán de Colima, Mexico, underwent its most intense eruptive phase since its Subplinian–Plinian 1913 AD eruption. Production of scoria coincident with elevated fumarolic activity and SO_2 flux indicate a significant switch of upper-conduit dynamics compared with the preceding decades of dome building and vulcanian explosions. A marked increase in rockfall events and degassing activity was observed on the 8th and 9th of July. On the 10th at 20:16 h (Local time = UTM − 6 h) a partial collapse of the dome generated a series of pyroclastic density currents (PDCs) that lasted 52 min and reached 9.1 km to the south of the volcano. The PDCs were mostly channelized by the Montegrande and San Antonio ravines, and produced a deposit with an estimated volume of 2.4×10^6 m^3. Nearly 16 h after the first collapse, a second and larger collapse occurred which lasted 1 h 47 min. This second collapse produced a series of PDCs along the same ravines, reaching a distance of 10.3 km. The total volume calculated for the PDCs of the second event is 8.0×10^6 m^3. Including associated ashfall deposits, the two episodes produced a total of 14.2×10^6 m^3 of fragmentary material. The collapses formed an amphitheater-shaped crater open towards the south. We propose that the dome collapse was triggered by arrival of gas-rich magma to the upper conduit, which then boiled-over and sustained the PDCs. A juvenile scoria sample selected from the second partial dome collapse contains hornblende, yet at an order of magnitude less abundant (0.2%) than that of 1913, and exhibits reaction rims, whereas the 1913 hornblende is unreacted. At present there is no compelling petrologic evidence for imminent end-cycle activity observed at Volcán de Colima.

1. Introduction

The andesitic stratovolcano Volcán de Colima in western México (19.51N, 103.62W, height 3860 m) is one of the most active volcanoes in North America and is currently in a highly active phase. There have been at least 29 significant eruptions since 1560 AD, according to historical accounts. Patterns within this activity are able to be identified (Luhr and Carmichael, 1980; Luhr et al., 2010; Crummy et al., 2014).

Luhr and Carmichael (1980) proposed that the second half of the historical eruptive record of Volcán de Colima (the last 440 years) can be characterized into cycles of activity. These cycles last around a century, and end with sub-Plinian to Plinian style eruption. Since the last 'end-cycle' eruptions were in 1818 and in 1913, it is therefore imperative to a) contextualize the current activity at Volcán de Colima, and b) develop methods to help predict imminent end-cycle activity. The focus of this communication is to describe the activity around the 10th and 11th July 2015, which represents the most intense eruption since 1913. We also try a non-routine method of petrologic characterization;

* Corresponding author.

http://dx.doi.org/10.1016/j.jvolgeores.2016.04.015

using X-ray micro-computed-tomography (XMT), for rapid petrologic assessment of volcanic products has the potential to hold value (Pankhust et al., 2014). In our particular case we focus upon rapidly estimating vesicle and crystal content.

2. Key context and real-time/near-real-time observations

2.1. Activity prior to the July events

In January 2013 Volcán de Colima showed signs of reactivation after nearly one and a half years in repose. A series of vulcanian explosions formed a small crater on the lava dome which had formed between 2007 and 2011 (Zobin et al., 2015). The explosions were followed by effusive activity. A new dome formed and rapidly filled the crater, overflowing towards the W, generating short lava flows.

Between March and October 2013 the flow rate was calculated to be 0.1 to 0.2 m^3/s. From October 2013 onwards, effusive activity was accompanied by minor explosive activity. This activity diminished until May and July 2014, when it increased suddenly, reaching a maximum of 1–2 m^3/s in September 2014 and fed two main lava flows headed towards the W and SW.

At this time, explosions were stronger when compared with those pre-July 2014. In particular, the explosion which occurred on November 21st generated block and ash flows towards the S, SW and W flanks, reaching lengths of up to 2.5 km. The SW lava flow had reached a length of over 2.3 km by the 4th of January 2015, with a volume of 11.7×10^6 m^3, while the W lava flow had reached a length of 1.5 km and a volume of ~5.8×10^6 m^3.

Explosive activity was particularly notable on the 3rd of January 2015, when an explosion occurred which generated 2 km long block and ash flows to the N flank. The summit dome was gradually destroyed by the explosions, creating ~35 m deep oval-shaped crater with long axis of ~200 m. Explosive activity subsequently decreased, yet the lava flows remained active until February.

Beginning in May 2015, a new dome was emplaced, and it covered the entire crater floor with an irregular rocky surface formed by lava blocks (cf. the usual steep-sided nature of previous domes). Small explosions were focused within the NE sector of the crater. During the night of 2nd July a moderate-large explosion occurred. The number and magnitude of explosions diminished significantly between the 3rd and the 7th of July (Fig. 1C).

Rockfalls started on the 3rd, and on the 7th of July two new lava flows were observed heading towards the N and SW, with lengths of ~620 and ~250 m respectively. Their emplacement was accompanied by frequent rockfalls that produced small block and ash flows. The estimated lava flow volume was 3.9×10^6 m^3.

The decrease in LP events in early July is real (Fig. 1D), and not the result of filtering out seismic signals of rockfalls and/or PDCs (note the offset by a few days before the substantial increase in rockfalls and PDCs).

Between the 8th and 9th of July a marked increase in the number of rockfalls (Fig. 1B) was observed. These correlated in time with a period of significant fumarolic activity visually observed near the summit during routine overflights, mostly on the S and E flanks. These observations

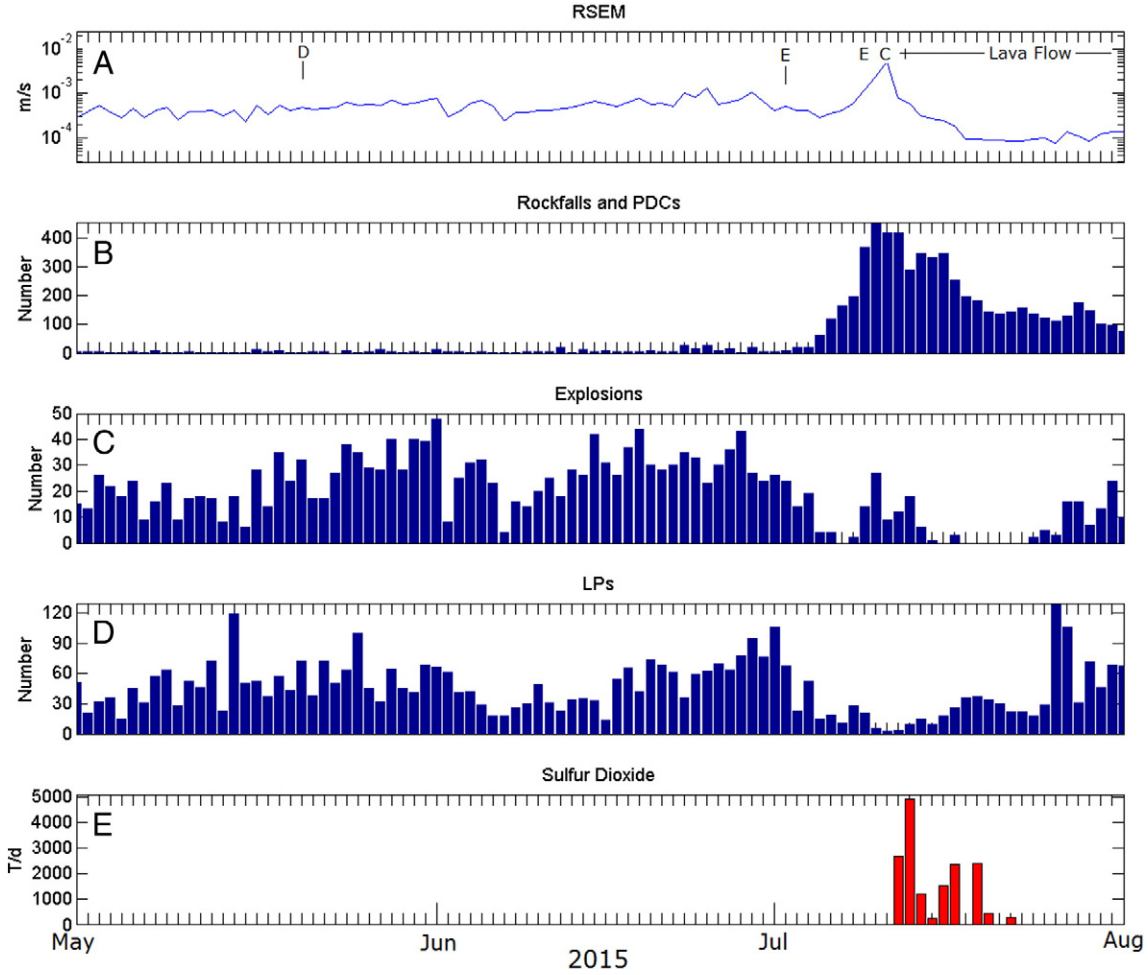

Fig. 1. A) RSEM. Daily number of events detected by automatic recognition based on Hidden Markov Models (HMMs, Benitez et al., 2009), B) rockfalls and PDCs, C) explosions, D) LPs, E) Sulfur dioxide measured with COSPEC starting on July 12th. 'D = Dome extrusion', 'E = moderate explosion', 'C = Lava dome collapse'.

are consistent with a further increase in the extrusion rate. At 11:16 h (Local time = UTM − 6 h) on the 9th, a vulcanian explosion generated a 7 km high (a.s.l.) ash column and small PDCs towards the S sector of the summit.

On the 10th of July a new ~200 m long lava flow was observed on the S flank of the volcano The increased fumarolic activity prevented observations of the summit dome. The rest of the day was characterized by an increase in the number and magnitude of rockfall events and associated PDCs, which reached up to 2.5 km from the vent. Until this moment, the overall behavior of Volcán de Colima was very similar to historical and recent lava domes and associated lava flow activity.

2.2. The PDCs of July 2015

2.2.1. The first event

At 20:16 h on the 10th July, a partial collapse of the dome occurred, which generated a series of much larger PDCs. These PDCs were mostly channelized by the Montegrande ravine on the S flank of the volcano where they reached 9.1 km in length (Fig. 2). The primary episode lasted 52 min (as illustrated by the seismic signal from the closest seismic station to the Montegrande ravine). A few PDCs were observed in the San Antonio ravine.

An ash cloud generated from the PDCs traveled W–NW to distances of up to ~150 km. Visual observations and seismic signal of this event show clearly that no eruptive column was associated with this process. Due to the strong winds and wet weather during the emplacement of the PDCs the W slopes were coated with ash, leaving the eastern slopes mostly ash free. The ash fall was in the form of accretionary lapilli (Fig. 3). In Zapotitlán de Vadillo, 21 km NW of the crater, ash was observed accumulated on vertical surfaces, another result of the prevailing humidity while the ash was falling.

Fig. 3. Accretionary lapilli of the July 10th ashfall as observed in La Yerbabuena village at 8 km from volcano.

The deposits were reconnoitered during an overflight the following morning. In some areas, small clustered circular crater-like structures were observed, which are described as secondary depositional processes in Stinton et al. (2014). Using the length and average cross-section dimensions of the ravine, we estimated a PDC deposit volume of 2.4×10^6 m^3, with a ±10% of error (240,000 m^3).

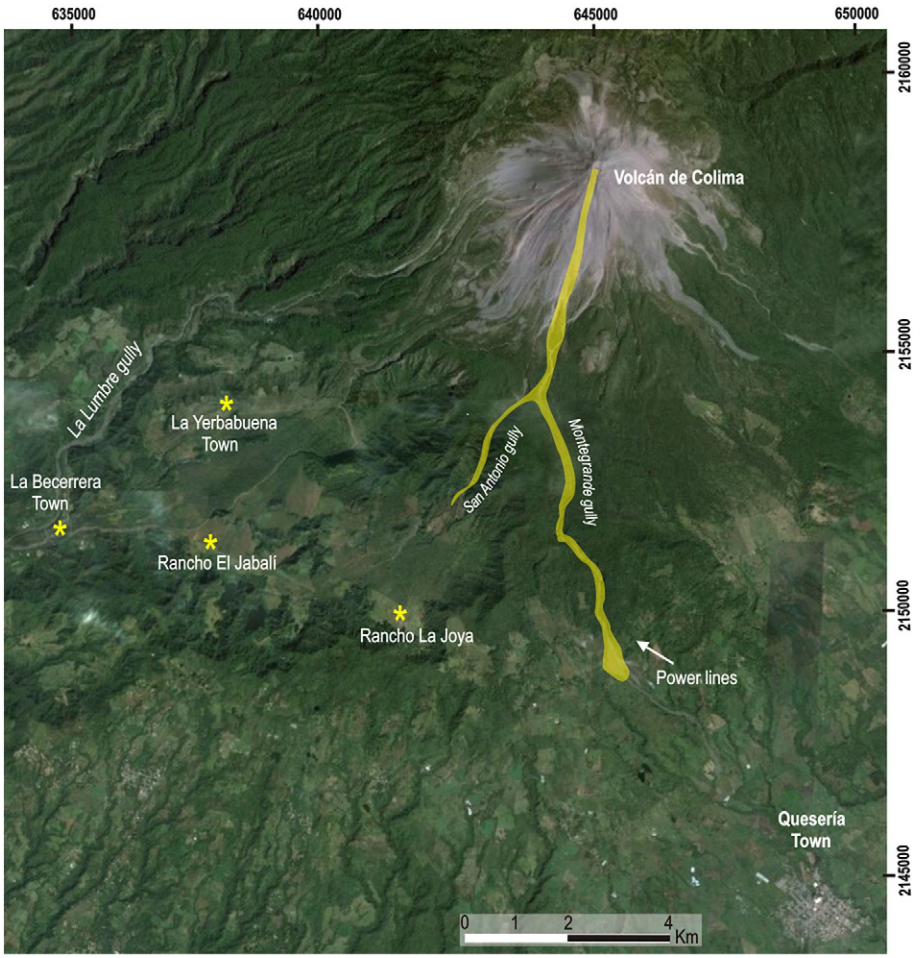

Fig. 2. Satellite image of Volcán de Colima and immediate surrounds, showing the distribution of the July 2015 PDCs along the Montegrande and San Antonio ravines.

2.2.2. The second event

At 11:58 h on the 11th, nearly 16 h after the first series of PDCs a second and considerably larger event commenced with similar characteristics. This lasted for 1 h and 47 min, and produced a series of PDCs which were emplaced along the same Montegrande ravine (Fig. 2). This event also did not produce an eruptive column (Fig. 4).

The deposit has a total length of 10.3 km, and reached a position where the ravine opens to a fan-shaped valley (Fig. 5, see also Fig. 2). This flow crossed the power lines of Comisión Federal de Electricidad (CFE), stopping ~370 m beyond and to a position 6 km from Quesería (Fig. 2), the nearest large town within this drainage. In the head of the Montegrande ravine the PDCs overtopped the divide with the San Antonio ravine, and advanced 2 km towards the La Joya and El Jabalí ranches, which are located ~6 km away from the crater (Fig. 2).

Ash generated by this event traveled in two directions at different altitudes. One plume traveled WNW (the typical wind direction) at high altitudes (>2.5 km a.s.l.), which reached similar long distances as the previous day's ash cloud. Ash was also dispersed to the S–SW by low level winds, and produced ashfall in the La Yerbabuena and La Becerrera villages (which evacuated voluntarily) located 8 and 12 km SW from the vent (Fig. 2), which accumulated a 0.5 cm ash deposit. Ashfall was also observed in the cities of Colima and Villa de Álvarez (32 km from the volcano).

The total volume calculated for the PDCs of the second event was 8.0×10^6 m^3. Including the ashfall, the first and second events produced a total of ~14.2×10^6 m^3 of fragmentary material with ±10% of error (1,420,000 m^3). Volumetrically minor PDCs were observed on the 12th, but had essentially stopped by the 13th.

2.3. Description of the deposits and their impact

In the days after these events deposits and areas affected were visually inspected. Field observations consistently demonstrated that while the dense portion of the PDCs remained channelized by the deep (~7–15 m) Montegrande ravine, whenever there is a change of ravine direction a dilute ash cloud surge decoupled from its PDC. The surge deposits are ~1–2 m thick at distances of up to 5 km from the vent. Decoupled ash continued in the direction of the preceding PDC path, traveled hundreds of meters farther down slope, and invaded the wooded slopes to distances of a few hundred meters.

The decoupled ash produced a large halo of thermal impact upon the forest, from total carbonization to slight discoloration. The second event blasted many trees which were incorporated into the flow and transported downhill to the flow front. Many trees along the Montegrande ravine margins were burnt. During later fieldwork it was noted that even after a month since deposition (about 2 m thick), the pyroclastic flow at the sample site was hot enough to combust pine resin upon tree trunks.

The deposits are poorly sorted, and all clasts are embedded in – and supported by – a mixed matrix of sand and ash sized particles. Careful rock-counting across the surface of the deposit from the second event reveals it to be comprised of 20–30% scoria clasts (from cm to >1 m in diameter). Scoria is atypical of material deposits of explosions at Volcán de Colima, and as such we consider its presence in such abundance to be highly significant. A representative sample of this juvenile scoria (sample VF-15-06) was collected on the afternoon of the 11th near the CFE power lines.

The remainder of the non-scoraceous clasts are dense andesite lithics which frequently display bread-crust textures. These lithics can reach size of >3 m width and this maximum size is present at the final front, 10.3 km from the vent. Their composition and texture is consistent with derivation from lava dome destruction, and are much more typical of fragmentary material from lava dome collapses during the past few decades.

2.4. Post-event observations of summit activity

During overflights of the volcano from the 13th July onwards, a number of post-event observations were made in the summit region. The scar left by the partial collapse of the summit dome and parts of the old crater wall were observed, shaped like an amphitheater (~100 m wide, ~180 m long and ~40 m high, for a calculated missing volume of nearly 7.2×10^5 m^3). The scar affected the feeder areas of

Fig. 4. Photograph of the second PDCs on July 11th, the absence of an eruptive column is clearly evident in this image. View from East.

Fig. 5. Aerial view, looking to the North, near the lower end of- and oblique to- Montegrande ravine. This photograph shows the new PDC deposits (center of image) in the context of Volcán de Colima and infrastructure. The two unvegetated parallel lines on the lower right of the image are corridors for CFE power lines.

the N and SW lava flows, while the lava flow to the S had been engulfed in the collapsed material.

A new lava flow had been emplaced, probably immediately after the collapse, and was being channelized by the amphitheater of the crater towards the S. This lava flow measured 2.1 km in length by July 20th, with an estimated volume of ~7.0 × 10^6 m^3. We calculate that it must have advanced at least 400 m/day and had a flow rate of 6 to 7 m^3/s, similar to the 2004 lava flow (Varley et al., 2010). This flow advanced until the 25th of August, having reached a total length of 2740 m and an estimated volume of 23.5 × 10^6 m^3 with ±10% of error (2,350,000 m^3).

Moderate explosive activity continued to the 11th August. This formed a wider and deeper amphitheater on the summit of nearly ~200 m in width and nearly ~50 m in depth. The open side of the crater is ~90 m wide (Fig. 6).

2.5. Significance of July 2015 events in remote sensing datasets

The RSEM 'Real-time Seismic Energy Measurement' value or Root Mean Square (RMS explained in De la Cruz-Reyna and Reyes-Dávila (2001) as measured at the closest seismic station from crater, was calculated daily from May until August (Fig. 1A). The July PDCs represent the maximum obtained since January 2013, and are among the highest values since monitoring began at this volcano (1989). It should be noted that the number and energy of rockfalls and PDCs during July 8th–12th dominate the seismic record. This noise obscures the automatic detection of LPs or explosions within this period (Fig. 1C–D).

The Geostationary Operational Environment Satellite system (GOES, http://goes.higp.hawaii.edu/volcanoes.shtml) detected a continuous hot spot (pixel 1 km^2) over the volcano between the 10th and the 30th of July. It, showed a high temperature in the crater area. This is best explained by the presence of the lava flow which was active during this period.

COSPEC retuned measurements of ~5000 t/d SO_2 starting on the 12th of July in response to the atypical eruption (Fig. 1E). Although this SO_2 degassing rate is lower than the highest recorded measurement on this volcano (20,000 t/d in 1998; Taran et al., 2002), these measurements are still considered remarkably high for this volcano that features a background flux <100 t/d (Taran et al., 2002).

Fig. 6. View of the summit before (4th February left) and after (11th August 2015, right) of the main activity of 10th–11th July. The open side of the crater is ~90 m. In both cases, the view is from SE to NW.

3. Implications of monitoring data

These large collapses and resulting PDCs represent a significant and sudden increase in intensity above background in all monitoring systems. Importantly, these events are also a departure from the dome-building and explosions style of activity. Together this set of observations appears to correlate with the Luhr and Carmichael (1990) model (wherein Volcán de Colima shows an apparent cyclicity of Plinian eruptions every 100 years), which by extension indicates that end-cycle activity is likely to occur imminently, and could be considered to have commenced with these events.

Independent datasets reflecting to intensive magmatic processes, including extremely high degassing rate and scoraceous juvenile material, point to a change in conduit dynamics. Arguably the most hazardous change would be a scenario of accelerated ascent rate, which may indicate an increase in eruptible magma mobilization. In order to investigate this possible causal factor further, we selected a representative sample of the juvenile scoria to analyze.

4. Context – and observations – of the juvenile scoria

Juvenile magma of the Sub-Plinian–Plinian 1913 eruption contained significant amounts of stable (no breakdown reaction rims) hornblende (with a model proportion of ~3.7%; Luhr and Carmichael, 1990). Volatiles are compatible in its structure, thus if hbl is in equilibrium with the host magma, in most cases the melt must contain >4.3 wt.% water (Rutherford and Hill, 1993; Moore and Carmichael, 1998; Carmichael, 2002). High magmatic water and its potential influence on magma explosivity is argued to be an important factor that explains the 1913 activity (Luhr, 2002; Savov et al., 2008).

The representative scoria sample (VF-15-06) from the second event preserves a several-cm wide banded texture of alternating pale-gray and dark-gray-matrix material. This is in contrast with typical lava-dome material which is dense, uniform in texture and color, and consistently interpreted as magma that had arrived in the upper conduit in a degassed state (e.g. Savov et al., 2008). Therefore this scoria sample represents the best opportunity to infer magmatic processes unrelated to dome-building.

Accordingly, there is reason to pay special attention to the presence and textural characteristics of hbl as indication of pre-eruptive magma water content. Scoria from the second event was observed in the field to contain significant phenocrysts of hbl. Should abundant and stable hbl be observed (i.e. euhedral grains in clear contact with glass or groundmass), this would substantiate an argument for the eruption of wet magma. It is important to note however, that the absence of hbl (or unstable hbl) does not substantiate a strong argument against wet magma.

VF-15-06 contains plag > opx > cpx > oxides > hbl (see Table 1) with crystal sizes from 5 mm to microlite set within banded matrix of devitrified groundmass. Mineral modes (see Table 1) were calculated using image analysis of a whole thin-section and individual major element maps (~55 million pixels). These maps were generated by routine energy dispersive spectroscopy (EDS) at the University of Leeds.

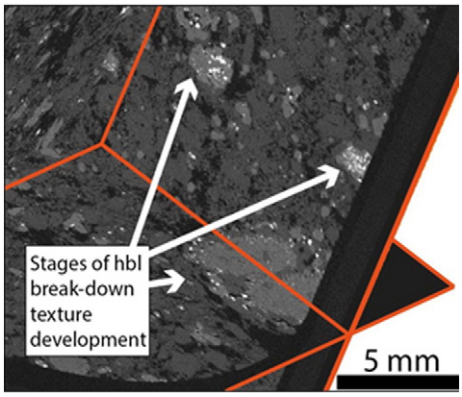

Fig. 7. Example of 3D X-ray microcomputed tomography data.

We found no textural evidence for the presence of fresh hbl. However, we did find textural evidence of two types of hbl breakdown reaction: narrow, fine grained and rim-only zones, and broad, pervasive and coarser grained zones. These appear to correlate with macrotexture of the sample, where the pervasive breakdown is found within dark-gray bands, and narrow rim breakdown within light-gray bands. Further work outside the scope of this study is required to confirm these observations before attaching significance further than to simply conclude that hbl is not stable in the July event scoria.

X-ray micro-tomography (XMT) data (generated at the Manchester X-ray Imaging Facility) provides a greater volume of sample to be observed with full three-dimensional context. This is a key advantage here given the rarity of hbl. It is also advantageous due to the rapid scanning capability of modern XMT systems which within a matter of hours, revealed evidence for hbl reaction (Fig. 7).

5. Discussion and interpretation

The marked increase in rockfall events on the 8th and 9th of July concomitant with elevated fumarolic activity preceded the strongest increase in effusion rate (dominated by the major events of the 10th and 11th of July). Together with the available SO_2 data this chronology suggests that high-level magmatic degassing, causing destabilization of the dome, was occurring immediately prior to the main PDCs. Considered alongside independent observations such as the lack of eruption column and the presence of fresh scoria within the PDC deposits, it is reasonable to link anomalous and transient bubble-rich magma to the physical behavior of the event.

As such we contend that the simplest explanation is that the arrival of a batch of comparatively bubble-rich magma triggered the initial dome collapse, and can point to physical behavior before and after

Table 1
VF-15-06 porosity and mineral modes using EDS image analysis, compared with other point-counted samples of recent lavas and 1913 scoria. Uncertainty on VF-15-06 modes are estimated at <0.01% (i.e. <10% absolute for hbl). Grains <30 μm^2 are not considered in bubble-free mineral modes and instead contribute to matrix.

% mode	July 2015 VF-15-06	1999 (n = 4)	1991 (n = 8)	1982 (n = 2)	1976 (n = 4)	1961–62 (n = 9)	1913 (n = 4)
Porosity	39.1						
Plagioclase	27.7	28.2	28.5	34.8	34.3	35.2	17.8
Clinopyroxene	2.8	4.6	4.9	5.6	3.8	3.5	3.4
Orthopyroxene	6.6	7.3	6.9	4.8	4.4	4.5	2.9
Hornblende	0.2	n/o	0.6	0.3	1.4	0.7	3.7
Fe/Ti-oxides	0.6	1.0	1.5	0.9	1.3	1.7	0.7
Olivine	n/o	n/o	0.2	n/o	0.4	0.1	n/o
Matrix	62.1	57.6	58.4	53.5	55.4	54.4	71.7
Total crystals	37.9	41.1	42.6	46.1	45.6	45.6	28.4
Cpx:Opx ratio	1:2.4	1:1.6	1:1.4	1:0.9	1:1.2	1:1.3	1:0.9
Total (bubble free)	100.0	98.7	100.9	99.6	101.0	100.1	100.2

1991 and 1999 values are averages of those reported in Luhr (2002). 1982–1913 values from Luhr and Carmichael (1990) and Luhr et al. (2010). n/o = not observed.

the event for continuity. The physical role of volatiles in the July 2015 events is in stark contrast to dome-building stages, including the prior ~6 months of explosions and lava flows. Finally, the lava flow emplaced after the collapses and PDC events can be simply explained by continued extrusion of the comparatively degassed portion of the same magma.

The PDCs are the largest volume since the 1913 eruption; their size likely played a role in the long distances reached. Importantly, the highly fluidized nature of the PDCs required to reach run-outs of >10 km, while carrying large clasts mobilized to the end of the PDC run-outs imply a significant and sustained load-carrying capacity. Large volumes of air were likely engulfed by – and contributed to – the PDC to achieve this capacity, which is a feature of boiling-over (Rader et al., 2015). The inclusion of both scoria and denser blocks exhibiting bread crust textures within an ash matrix bear the textural hallmarks of boiling-over (Sulpizio et al., 2014; Rader et al., 2015; Dufek et al., 2015). Entrainment and heating of air leading to extensive elutriation helps explain the widespread ash cloud surge, similar to that observed at Tungurahua volcano in the 2006 events (Hall et al., 2013).

Does the juvenile component of the July event PDCs appear similar to the 1913 magma?

Total porosity of the scoria sample is ~39%, which is in contrast to that exhibited by typical dense lava-dome samples (Savov et al., 2008), and more similar to the juvenile 1913 deposits. Total crystallinity is ~38% and is the lowest since 1913. However the *assemblage* appears most similar to that of lavas from the previous ~50 years of extrusion (see Table 1), albeit with less cpx and Fe-oxides. Opx and plag abundances however, are both significantly greater than opx and plag abundance within the 1913 Sub-Plinian-juvenile material (Luhr and Carmichael, 1990).

While some mineralogical variability is observed across a decadal timeframe, hbl is conspicuously low in abundance (~0.2%). This is an order of magnitude less abundant than that of 1913 scoria (Luhr and Carmichael, 1990). Furthermore, we have not observed stable hbl in this representative sample.

The simplest petrologic interpretation is that the scoria represents the same magma as the lava-dome building material, and not magma similar to the 1913. The differences in the volatile content and total crystallinity can be explained by the lava dome samples experiencing longer degassing and accompanying crystallization (Savov et al., 2008).

These events may simply demonstrate an end-member example of normal variation within this phase of activity. Since we have not observed this intensity before, the scale of the PDCs were unexpected and linked to end-cycle activity. We note, however, that comparisons to material erupted in the lead-up to the 1913 end-cycle eruption is not possible — there appears to be no preserved record, and as such we cannot rule out the possibility that this anomalous PDC itself may represent lead-indication of end-cycle activity.

Petrologic work reveals that the only parameters approaching similarity with 1913 magma is that of the scoraceous (bubble-rich) nature and total crystallinity. Both of these parameters strongly influence the physical nature of magma which help explain the July events status as the longest PDC at Volcán de Colima since 1913. Because the mineral modes and ratios are considerably different we cannot suggest a similar petrogenesis, and thus similarities are likely to be governed by upper conduit physical dynamics as opposed to deep-seated magmatic processes.

6. Conclusions

We favor a boiling-over mechanism to explain the anomalous eruptions of July 2015 at Volcán de Colima. Arrival of an undegassed magma batch in the upper conduit displaced the dome in two principal events. This magma continued to ascend and feed PDCs which impacted the surrounding region on a scale not observed since the 1913 end-cycle eruption. To date there is no compelling evidence to support a mechanistic comparison between these events and the last end-cycle eruption in 1913. Further work is required to ascertain whether these events signify an anomalous magma batch during a period of dome-building, a change in upper conduit dynamics, or a fundamental switch in plumbing system regime that may lead to end-cycle activity.

Acknowledgments

We appreciate the support provided by Unidad Estatal de Protección Civil del Estado de Colima, Unidad Estatal de Protección Civil del Estado de Jalisco, Coordinación Nacional de Protección Civil and Policía Federal. MJP gratefully acknowledges the support of an AXA Research Fund Postdoctoral Fellowship. Richard Walshaw, Lesley Neve and Sara Nonni are thanked for analytical assistance.

This work was made possible by the facilities and support provided by the Research Complex at Harwell, funded in part by the EPSRC (EP/I02249X/1).

References

Benitez, M.C., Lesage, P., Cortés, G., Segura, J.C., Ibáñez, J.M., De la Torre, A., 2009. Automatic recognition of volcanic–seismic events based on Continuous Hidden Markov Models. In: Bean, C.J., Braiden, A.K., Lokmer, I., Martini, F., O'Brien, G.S. (Eds.), The VOLUME Project, VOLcanoes: Understanding Subsurface Mass MoveMEnt, pp. 130–139.

Carmichael, I.S.E., 2002. The andesite aqueduct: perspectives on the evolution of intermediate magmatism in west-central (105–99°W) Mexico. Contrib. Mineral. Petrol. 143, 641–663.

Crummy, J., Savov, I.P., Navarro-Ochoa, C., Morgan, D., Wilson, M., 2014. High-K mafic Plinian eruptions of Volcán de Colima, México. J. Petrology 55 (10), 1–18.

De la Cruz-Reyna, S., Reyes-Dávila, G.A., 2001. A model to describe precursory material failure phenomena: application to short-term forecasting at Colima volcano, Mexico. Bull. Volcanol. 63, 297–308.

Dufek, J., Esposti Ongaro, T., Roche, O., 2015. Pyroclastic density currents: processes and models. Chapter 35. In: Sigurdsson, H., Loughton, B., McNutt, S., Rymer, H., Stix, J. (Eds.), Part IV Explosive Volcanism, The Encyclopedia of Volcanoes, second ed., p. 620 (2015).

Hall, M.L., Steele, A.L., Mothes, P.A., Ruiz, M.C., 2013. Pyroclastic density currents (PDC) of the 16–17 August 2006 eruptions of Tungurahua volcano, Ecuador: geophysical registry and characteristics. J. Volcanol. Geotherm. Res. 265, 78–93 (2013).

Luhr, J.F., 2002. Petrology and geochemistry of the 1991 and 1998–1999 lava flows from Volcán de Colima, México: implications for the end of the current eruptive cycle. J. Volcanol. Geotherm. Res. 117 (1–2), 169–194.

Luhr, J.F., Carmichael, I.S.E., 1980. The Colima Volcanic Complex, México: part I. Post caldera andesites from Volcán Colima. Contrib. Mineral. Petrol. 71, 343–372.

Luhr, J.F., Carmichael, I.S.E., 1990. Petrological monitoring of cyclical eruptive activity at Volcán de Colima, Mexico. J. Volcanol. Geotherm. Res. 42 (3), 235–260.

Luhr, J.F., Navarro-Ochoa, C., Savov, I.P., 2010. Tephrochronology, petrology and geochemistry of Late-Holocene pyroclast deposits from Volcán de Colima, Mexico. J. Volcanol. Geotherm. Res. 197, 1–32.

Moore, G.M., Carmichael, I.S.E., 1998. The hydrous phase equilibria (to 3 kbar) of an andesite and basaltic andesite from western Mexico: constraints on water content and conditions of phenocryst growth. Contrib. Mineral. Petrol. 130, 304–319.

Pankhust, M.J., Dobson, K.J., Morgan, D.J., Loughlin, S.C., Thordarson, Th., Lee, P.D., Courtois, L., 2014. Monitoring the magmas fuelling volcanic eruptions in near-real-time using X-ray micro-computed tomography. J. Petrol. 55 (3), 671–684.

Rader, E., Geist, D., Geissman, J., Dufek, J., Harpp, K., 2015. Hot clast and cold blast: thermal heterogeneity in boiling-over pyroclastic density currents. The Use of Paleomagnetism and Rock Magnetism to Understand Volcanic ProcessesGeological Society Publication 396. IAVCEI, pp. 67–87.

Rutherford, M.J., Hill, P.M., 1993. Magma ascent rates from amphibole breakdown: an experimental study applied to the 1980–1986 Mount St. Helens eruptions. J. Geophys. Res. 98 (19), 667–19,685.

Savov, I.P., Luhr, J.F., Navarro-Ochoa, C., 2008. Petrology and geochemistry of lava and ash erupted from Volcán Colima, Mexico, during 1998–2005. J. Volcanol. Geotherm. Res. 174 (4), 241–256.

Stinton, A.J., Cole, P.D., Odbert, H.M., Christopher, T., Avard, G., Bernstein, M., 2014. Dome growth and valley fill during Phase 5 (8 October 2009–11 February 2010) at the Soufrière Hill Volcano, Montserrat. In: Wadge, G., Robertson, R.E.A., Voight, B. (Eds.), The Eruption of Soufriere Hills Volcano, Montserrat from 2000 to 2010. Geological Society, London, Memoirs 39, pp. 113–131.

Sulpizio, R., Dellino, P., Doronzo, D.M., Sarocchi, D., 2014. Pyroclastic density currents: state of the art and perspectives. J. Volcanol. Geotherm. Res. 283, 36–65.

Taran, Y., Gavilanes-Ruiz, J.C., Corte.s, A., 2002. Chemical and isotopic composition of fumarolic gases and the SO_2 flux from Volcán de Colima, México, between 1994 and 1998 eruptions. J. Volcanol. Geotherm. Res. 117, 105–119.

Varley, N., Arámbula-Mendoza, R., Reyes-Dávila, G., Stevenson, J., Harwood, R., 2010. Long-period seismicity during magma movement at Volcán de Colima. Bull. Volcanol. 72, 1093–1107.

Zobin, V.M., Arámbula, R., Bretón, M., Reyes, G., Plascencia, I., Navarro, C., Téllez, A., Campos, A., González, M., León, Z., Martínez, A., Ramírez, C., 2015. Dynamics of the January 2013–June 2014 explosive–effusive episode in the eruption of Volcán de Colima, México: insights from seismic and video monitoring. Bull. Volcanol. 77, 1–13.